BABAR-PUB-13/020
SLAC-PUB-15925

arXiv:1403.4409v1 [hep-ex] 18 Mar 2014

Antideuteron production in $\Upsilon(nS)$ decays and in $e^+e^- \to q\bar{q}$ at $\sqrt{s} \approx 10.58\,\mathrm{GeV}$

J. P. Lees,[1] V. Poireau,[1] V. Tisserand,[1] E. Grauges,[2] A. Palano[ab],[3] G. Eigen,[4] B. Stugu,[4] D. N. Brown,[5] L. T. Kerth,[5] Yu. G. Kolomensky,[5] M. J. Lee,[5] G. Lynch,[5] H. Koch,[6] T. Schroeder,[6] C. Hearty,[7] T. S. Mattison,[7] J. A. McKenna,[7] R. Y. So,[7] A. Khan,[8] V. E. Blinov[ac],[9] A. R. Buzykaev[a],[9] V. P. Druzhinin[ab],[9] V. B. Golubev[ab],[9] E. A. Kravchenko[ab],[9] A. P. Onuchin[ac],[9] S. I. Serednyakov[ab],[9] Yu. I. Skovpen[ab],[9] E. P. Solodov[ab],[9] K. Yu. Todyshev[ab],[9] A. J. Lankford,[10] M. Mandelkern,[10] B. Dey,[11] J. W. Gary,[11] O. Long,[11] C. Campagnari,[12] M. Franco Sevilla,[12] T. M. Hong,[12] D. Kovalskyi,[12] J. D. Richman,[12] C. A. West,[12] A. M. Eisner,[13] W. S. Lockman,[13] W. Panduro Vazquez,[13] B. A. Schumm,[13] A. Seiden,[13] D. S. Chao,[14] C. H. Cheng,[14] B. Echenard,[14] K. T. Flood,[14] D. G. Hitlin,[14] T. S. Miyashita,[14] P. Ongmongkolkul,[14] F. C. Porter,[14] R. Andreassen,[15] Z. Huard,[15] B. T. Meadows,[15] B. G. Pushpawela,[15] M. D. Sokoloff,[15] L. Sun,[15] P. C. Bloom,[16] W. T. Ford,[16] A. Gaz,[16] J. G. Smith,[16] S. R. Wagner,[16] R. Ayad,[17,a] W. H. Toki,[17] B. Spaan,[18] D. Bernard,[19] M. Verderi,[19] S. Playfer,[20] D. Bettoni[a],[21] C. Bozzi[a],[21] R. Calabrese[ab],[21] G. Cibinetto[ab],[21] E. Fioravanti[ab],[21] I. Garzia[ab],[21] E. Luppi[ab],[21] L. Piemontese[a],[21] V. Santoro[a],[21] A. Calcaterra,[22] R. de Sangro,[22] G. Finocchiaro,[22] S. Martellotti,[22] P. Patteri,[22] I. M. Peruzzi,[22,b] M. Piccolo,[22] M. Rama,[22] A. Zallo,[22] R. Contri[ab],[23] M. Lo Vetere[ab],[23] M. R. Monge[ab],[23] S. Passaggio[a],[23] C. Patrignani[ab],[23] E. Robutti[a],[23] B. Bhuyan,[24] V. Prasad,[24] M. Morii,[25] A. Adametz,[26] U. Uwer,[26] H. M. Lacker,[27] P. D. Dauncey,[28] U. Mallik,[29] C. Chen,[30] J. Cochran,[30] S. Prell,[30] H. Ahmed,[31] A. V. Gritsan,[32] N. Arnaud,[33] M. Davier,[33] D. Derkach,[33] G. Grosdidier,[33] F. Le Diberder,[33] A. M. Lutz,[33] B. Malaescu,[33,c] P. Roudeau,[33] A. Stocchi,[33] G. Wormser,[33] D. J. Lange,[34] D. M. Wright,[34] J. P. Coleman,[35] J. R. Fry,[35] E. Gabathuler,[35] D. E. Hutchcroft,[35] D. J. Payne,[35] C. Touramanis,[35] A. J. Bevan,[36] F. Di Lodovico,[36] R. Sacco,[36] G. Cowan,[37] J. Bougher,[38] D. N. Brown,[38] C. L. Davis,[38] A. G. Denig,[39] M. Fritsch,[39] W. Gradl,[39] K. Griessinger,[39] A. Hafner,[39] E. Prencipe,[39] K. R. Schubert,[39] R. J. Barlow,[40,d] G. D. Lafferty,[40] R. Cenci,[41] B. Hamilton,[41] A. Jawahery,[41] D. A. Roberts,[41] R. Cowan,[42] G. Sciolla,[42] R. Cheaib,[43] P. M. Patel,[43,e] S. H. Robertson,[43] N. Neri[a],[44] F. Palombo[ab],[44] L. Cremaldi,[45] R. Godang,[45,f] P. Sonnek,[45] D. J. Summers,[45] M. Simard,[46] P. Taras,[46] G. De Nardo[ab],[47] G. Onorato[ab],[47] C. Sciacca[ab],[47] M. Martinelli,[48] G. Raven,[48] C. P. Jessop,[49] J. M. LoSecco,[49] K. Honscheid,[50] R. Kass,[50] E. Feltresi[ab],[51] M. Margoni[ab],[51] M. Morandin[a],[51] M. Posocco[a],[51] M. Rotondo[a],[51] G. Simi[ab],[51] F. Simonetto[ab],[51] R. Stroili[ab],[51] S. Akar,[52] E. Ben-Haim,[52] M. Bomben,[52] G. R. Bonneaud,[52] H. Briand,[52] G. Calderini,[52] J. Chauveau,[52] Ph. Leruste,[52] G. Marchiori,[52] J. Ocariz,[52] S. Sitt,[52] M. Biasini[ab],[53] E. Manoni[a],[53] S. Pacetti[ab],[53] A. Rossi[a],[53] C. Angelini[ab],[54] G. Batignani[ab],[54] S. Bettarini[ab],[54] M. Carpinelli[ab],[54,g] G. Casarosa[ab],[54] A. Cervelli[ab],[54] M. Chrzaszcz[ab],[54] F. Forti[ab],[54] M. A. Giorgi[ab],[54] A. Lusiani[ac],[54] B. Oberhof[ab],[54] E. Paoloni[ab],[54] A. Perez[a],[54] G. Rizzo[ab],[54] J. J. Walsh[a],[54] D. Lopes Pegna,[55] J. Olsen,[55] A. J. S. Smith,[55] R. Faccini[ab],[56] F. Ferrarotto[a],[56] F. Ferroni[ab],[56] M. Gaspero[ab],[56] L. Li Gioi[a],[56] G. Piredda[a],[56] C. Bünger,[57] S. Dittrich,[57] O. Grünberg,[57] T. Hartmann,[57] T. Leddig,[57] C. Voß,[57] R. Waldi,[57] T. Adye,[58] E. O. Olaiya,[58] F. F. Wilson,[58] S. Emery,[59] G. Vasseur,[59] F. Anulli,[60,h] D. Aston,[60] D. J. Bard,[60] C. Cartaro,[60] M. R. Convery,[60] J. Dorfan,[60] G. P. Dubois-Felsmann,[60] W. Dunwoodie,[60] M. Ebert,[60] R. C. Field,[60] B. G. Fulsom,[60] M. T. Graham,[60] C. Hast,[60] W. R. Innes,[60] P. Kim,[60] D. W. G. S. Leith,[60] P. Lewis,[60] D. Lindemann,[60] S. Luitz,[60] V. Luth,[60] H. L. Lynch,[60] D. B. MacFarlane,[60] D. R. Muller,[60] H. Neal,[60] M. Perl,[60] T. Pulliam,[60] B. N. Ratcliff,[60] A. Roodman,[60] A. A. Salnikov,[60] R. H. Schindler,[60] A. Snyder,[60] D. Su,[60] M. K. Sullivan,[60] J. Va'vra,[60] A. P. Wagner,[60] W. F. Wang,[60] W. J. Wisniewski,[60] H. W. Wulsin,[60] M. V. Purohit,[61] R. M. White,[61,i] J. R. Wilson,[61] A. Randle-Conde,[62] S. J. Sekula,[62] M. Bellis,[63] P. R. Burchat,[63] E. M. T. Puccio,[63] M. S. Alam,[64] J. A. Ernst,[64] R. Gorodeisky,[65] N. Guttman,[65] D. R. Peimer,[65] A. Soffer,[65] S. M. Spanier,[66] J. L. Ritchie,[67] A. M. Ruland,[67] R. F. Schwitters,[67] B. C. Wray,[67] J. M. Izen,[68] X. C. Lou,[68] F. Bianchi[ab],[69] F. De Mori[ab],[69] A. Filippi[a],[69] D. Gamba[ab],[69] L. Lanceri[ab],[70] L. Vitale[ab],[70] F. Martinez-Vidal,[71] A. Oyanguren,[71] P. Villanueva-Perez,[71] J. Albert,[72] Sw. Banerjee,[72] A. Beaulieu,[72] F. U. Bernlochner,[72] H. H. F. Choi,[72] G. J. King,[72] R. Kowalewski,[72] M. J. Lewczuk,[72] T. Lueck,[72] I. M. Nugent,[72] J. M. Roney,[72] R. J. Sobie,[72] N. Tasneem,[72] T. J. Gershon,[73] P. F. Harrison,[73] T. E. Latham,[73] H. R. Band,[74] S. Dasu,[74] Y. Pan,[74] R. Prepost,[74] and S. L. Wu[74]

(The *BABAR* Collaboration)

[1] *Laboratoire d'Annecy-le-Vieux de Physique des Particules (LAPP),*

Université de Savoie, CNRS/IN2P3, F-74941 Annecy-Le-Vieux, France
[2] *Universitat de Barcelona, Facultat de Fisica, Departament ECM, E-08028 Barcelona, Spain*
[3] *INFN Sezione di Bari[a]; Dipartimento di Fisica, Università di Bari[b], I-70126 Bari, Italy*
[4] *University of Bergen, Institute of Physics, N-5007 Bergen, Norway*
[5] *Lawrence Berkeley National Laboratory and University of California, Berkeley, California 94720, USA*
[6] *Ruhr Universität Bochum, Institut für Experimentalphysik 1, D-44780 Bochum, Germany*
[7] *University of British Columbia, Vancouver, British Columbia, Canada V6T 1Z1*
[8] *Brunel University, Uxbridge, Middlesex UB8 3PH, United Kingdom*
[9] *Budker Institute of Nuclear Physics SB RAS, Novosibirsk 630090[a],*
Novosibirsk State University, Novosibirsk 630090[b],
Novosibirsk State Technical University, Novosibirsk 630092[c], Russia
[10] *University of California at Irvine, Irvine, California 92697, USA*
[11] *University of California at Riverside, Riverside, California 92521, USA*
[12] *University of California at Santa Barbara, Santa Barbara, California 93106, USA*
[13] *University of California at Santa Cruz, Institute for Particle Physics, Santa Cruz, California 95064, USA*
[14] *California Institute of Technology, Pasadena, California 91125, USA*
[15] *University of Cincinnati, Cincinnati, Ohio 45221, USA*
[16] *University of Colorado, Boulder, Colorado 80309, USA*
[17] *Colorado State University, Fort Collins, Colorado 80523, USA*
[18] *Technische Universität Dortmund, Fakultät Physik, D-44221 Dortmund, Germany*
[19] *Laboratoire Leprince-Ringuet, Ecole Polytechnique, CNRS/IN2P3, F-91128 Palaiseau, France*
[20] *University of Edinburgh, Edinburgh EH9 3JZ, United Kingdom*
[21] *INFN Sezione di Ferrara[a]; Dipartimento di Fisica e Scienze della Terra, Università di Ferrara[b], I-44122 Ferrara, Italy*
[22] *INFN Laboratori Nazionali di Frascati, I-00044 Frascati, Italy*
[23] *INFN Sezione di Genova[a]; Dipartimento di Fisica, Università di Genova[b], I-16146 Genova, Italy*
[24] *Indian Institute of Technology Guwahati, Guwahati, Assam, 781 039, India*
[25] *Harvard University, Cambridge, Massachusetts 02138, USA*
[26] *Universität Heidelberg, Physikalisches Institut, D-69120 Heidelberg, Germany*
[27] *Humboldt-Universität zu Berlin, Institut für Physik, D-12489 Berlin, Germany*
[28] *Imperial College London, London, SW7 2AZ, United Kingdom*
[29] *University of Iowa, Iowa City, Iowa 52242, USA*
[30] *Iowa State University, Ames, Iowa 50011-3160, USA*
[31] *Physics Department, Jazan University, Jazan 22822, Kingdom of Saudia Arabia*
[32] *Johns Hopkins University, Baltimore, Maryland 21218, USA*
[33] *Laboratoire de l'Accélérateur Linéaire, IN2P3/CNRS et Université Paris-Sud 11,*
Centre Scientifique d'Orsay, F-91898 Orsay Cedex, France
[34] *Lawrence Livermore National Laboratory, Livermore, California 94550, USA*
[35] *University of Liverpool, Liverpool L69 7ZE, United Kingdom*
[36] *Queen Mary, University of London, London, E1 4NS, United Kingdom*
[37] *University of London, Royal Holloway and Bedford New College, Egham, Surrey TW20 0EX, United Kingdom*
[38] *University of Louisville, Louisville, Kentucky 40292, USA*
[39] *Johannes Gutenberg-Universität Mainz, Institut für Kernphysik, D-55099 Mainz, Germany*
[40] *University of Manchester, Manchester M13 9PL, United Kingdom*
[41] *University of Maryland, College Park, Maryland 20742, USA*
[42] *Massachusetts Institute of Technology, Laboratory for Nuclear Science, Cambridge, Massachusetts 02139, USA*
[43] *McGill University, Montréal, Québec, Canada H3A 2T8*
[44] *INFN Sezione di Milano[a]; Dipartimento di Fisica, Università di Milano[b], I-20133 Milano, Italy*
[45] *University of Mississippi, University, Mississippi 38677, USA*
[46] *Université de Montréal, Physique des Particules, Montréal, Québec, Canada H3C 3J7*
[47] *INFN Sezione di Napoli[a]; Dipartimento di Scienze Fisiche,*
Università di Napoli Federico II[b], I-80126 Napoli, Italy
[48] *NIKHEF, National Institute for Nuclear Physics and High Energy Physics, NL-1009 DB Amsterdam, The Netherlands*
[49] *University of Notre Dame, Notre Dame, Indiana 46556, USA*
[50] *Ohio State University, Columbus, Ohio 43210, USA*
[51] *INFN Sezione di Padova[a]; Dipartimento di Fisica, Università di Padova[b], I-35131 Padova, Italy*
[52] *Laboratoire de Physique Nucléaire et de Hautes Energies,*
IN2P3/CNRS, Université Pierre et Marie Curie-Paris6,
Université Denis Diderot-Paris7, F-75252 Paris, France
[53] *INFN Sezione di Perugia[a]; Dipartimento di Fisica, Università di Perugia[b], I-06123 Perugia, Italy*
[54] *INFN Sezione di Pisa[a]; Dipartimento di Fisica,*
Università di Pisa[b]; Scuola Normale Superiore di Pisa[c], I-56127 Pisa, Italy
[55] *Princeton University, Princeton, New Jersey 08544, USA*
[56] *INFN Sezione di Roma[a]; Dipartimento di Fisica,*
Università di Roma La Sapienza[b], I-00185 Roma, Italy

[57] Universität Rostock, D-18051 Rostock, Germany
[58] Rutherford Appleton Laboratory, Chilton, Didcot, Oxon, OX11 0QX, United Kingdom
[59] CEA, Irfu, SPP, Centre de Saclay, F-91191 Gif-sur-Yvette, France
[60] SLAC National Accelerator Laboratory, Stanford, California 94309 USA
[61] University of South Carolina, Columbia, South Carolina 29208, USA
[62] Southern Methodist University, Dallas, Texas 75275, USA
[63] Stanford University, Stanford, California 94305-4060, USA
[64] State University of New York, Albany, New York 12222, USA
[65] Tel Aviv University, School of Physics and Astronomy, Tel Aviv, 69978, Israel
[66] University of Tennessee, Knoxville, Tennessee 37996, USA
[67] University of Texas at Austin, Austin, Texas 78712, USA
[68] University of Texas at Dallas, Richardson, Texas 75083, USA
[69] INFN Sezione di Torino[a]; Dipartimento di Fisica, Università di Torino[b], I-10125 Torino, Italy
[70] INFN Sezione di Trieste[a]; Dipartimento di Fisica, Università di Trieste[b], I-34127 Trieste, Italy
[71] IFIC, Universitat de Valencia-CSIC, E-46071 Valencia, Spain
[72] University of Victoria, Victoria, British Columbia, Canada V8W 3P6
[73] Department of Physics, University of Warwick, Coventry CV4 7AL, United Kingdom
[74] University of Wisconsin, Madison, Wisconsin 53706, USA

We present measurements of the inclusive production of antideuterons in e^+e^- annihilation into hadrons at ≈ 10.58 GeV center-of-mass energy and in $\Upsilon(1S, 2S, 3S)$ decays. The results are obtained using data collected by the *BABAR* detector at the PEP-II electron-positron collider. Assuming a fireball spectral shape for the emitted antideuteron momentum, we find $\mathcal{B}(\Upsilon(1S) \to \bar{d}X) = (2.81 \pm 0.49(\mathrm{stat})^{+0.20}_{-0.24}(\mathrm{syst})) \times 10^{-5}$, $\mathcal{B}(\Upsilon(2S) \to \bar{d}X) = (2.64 \pm 0.11(\mathrm{stat})^{+0.26}_{-0.21}(\mathrm{syst})) \times 10^{-5}$, $\mathcal{B}(\Upsilon(3S) \to \bar{d}X) = (2.33 \pm 0.15(\mathrm{stat})^{+0.31}_{-0.28}(\mathrm{syst})) \times 10^{-5}$, and $\sigma(e^+e^- \to \bar{d}X) = (9.63 \pm 0.41(\mathrm{stat})^{+1.17}_{-1.01}(\mathrm{syst}))$ fb.

PACS numbers: 13.60.Rj, 13.87.Fh, 13.25.Gv

The production of nuclei and anti-nuclei in hadronic collisions and in hadronization processes has recently attracted considerable theoretical and experimental interest [1–3], since cosmic anti-nuclei may provide a sensitive probe of dark matter annihilation. Dark matter particles might annihilate into two colored partons – quarks (q) and gluons (g) – which could hadronize into mesons and baryons, potentially forming bound states such as light (anti)nuclei. The latter process, requiring at least six q or $\overline{q}$ in close proximity, is poorly understood both theoretically and experimentally, and precise measurements of both total rates and momentum spectra are needed. With no initial-state hadrons, e^+e^- annihilations provide a clean probe of this process not only for q and $\overline{q}$ but also for g via decays of Υ and other vector resonances.

Experimental measurements focus on antideuteron ($\overline{d}$) production as such studies are not limited, as in the deuteron (d) production case, by the high nuclei background due to interactions with the detector materials. The ARGUS [4] and CLEO [5] experiments observed $\overline{d}$ production at the level of 3×10^{-5} per $\Upsilon(1S)$ and $\Upsilon(2S)$ decays, and set limits on production in $\Upsilon(4S)$ decays and $e^+e^- \to q\overline{q}$ at 10.6 GeV. The ALEPH [6] experiment observed a 3σ evidence for $\overline{d}$ production in $e^+e^- \to q\overline{q}$ at 91.2 GeV. In these measurements, the accessible kinematic range, 0.4 – 1.7 GeV/c, was representing less than 20% of the phase space where d and $\overline{d}$ could be identified.

In this Letter, we present studies of $\overline{d}$ production in e^+e^- annihilation data taken on and just below the $\Upsilon(2S)$, $\Upsilon(3S)$ and $\Upsilon(4S)$ resonances. We also study the $\overline{d}$ production from $\Upsilon(1S)$ using the $\Upsilon(2S) \to \Upsilon(1S)\pi^+\pi^-$ decay chain. The boost of the CM allows a wide momentum to be accessed, 0.3 – 3 GeV/c, which corresponds to 0.5 – 1.5 GeV/c in the laboratory frame. We confirm the $\Upsilon(1S)$ rates, improve the coverage and precision for $\Upsilon(2S)$ decays, measure $\overline{d}$ production in $\Upsilon(3S)$ decays, and also, for the first time, in $e^+e^- \to q\overline{q}$ near 10.6 GeV.

The results presented here are obtained from the complete *BABAR* $\Upsilon(2S, 3S, 4S)$ ($\Upsilon(nS)$) datasets (Onpeak), including data collected at a CM energy 40 MeV below the peak of each resonance (Offpeak). The luminosity [7] collected for each dataset and the corresponding number of $\Upsilon(nS)$ decays are reported in Table I. We also use Monte Carlo (MC) simulated data samples generated using JETSET [8] for $e^+e^- \to q\overline{q}\,(q = u, d, s)$ events and EVTGEN [9] for $\Upsilon(nS)$ decays. The interaction of simulated particles with the *BABAR* detector is modeled using GEANT4 [10]. Neither d nor $\overline{d}$ production is implemented in JETSET, and $\overline{d}$ cannot be simulated in the version of GEANT4 that is used. Therefore we use the EVTGEN phase-space generator and GEANT4 to simulate $\Upsilon(2S, 3S) \to d\bar{N}\bar{N}'(5h)$ decays (where h indicates a

TABLE I. Collected luminosity and number of decays for the samples used in the analysis. Integrated luminosity is reported both for the Onpeak and Offpeak samples.

Resonance	**Onpeak**	**# of Υ Decays**	**Offpeak**
$\Upsilon(4S)$	$429\,\mathrm{fb}^{-1}$	463×10^6	$44.8\,\mathrm{fb}^{-1}$
$\Upsilon(3S)$	$28.5\,\mathrm{fb}^{-1}$	116×10^6	$2.63\,\mathrm{fb}^{-1}$
$\Upsilon(2S)$	$14.4\,\mathrm{fb}^{-1}$	98.3×10^6	$1.50\,\mathrm{fb}^{-1}$

$K^{\pm}$, $\pi^{\pm}$, or π^0, and $N, N' = p, n$) and $e^+e^- \to q\overline{q} \to d\bar{N}\bar{N}'(5h)$ events for studying reconstruction efficiencies. The additional five hadrons are a representative average of additional particles in the decay and restrict the phase-space, so we have d's with CM momentum lower than 3 GeV/c. These samples will be referred to as "signal MC" throughout this Letter. To account for differences between data and MC samples, corrections are applied and systematic uncertainties are assigned, as discussed below.

The *BABAR* detector, trigger, and the coordinate system used throughout, are described in detail in Refs. [11, 12]. The most relevant part of the detector for this analysis is the tracking system, composed of a 5-layer inner silicon strip tracker, the Silicon Vertex Tracker (SVT), and the 40-layer small-cell Drift Chamber (DCH) inside a 1.5 Tesla axial magnetic field. The SVT provides information on track parameters near the interaction point (IP), while the DCH has a 98% efficiency for detecting charged particles with $p_T > 500\,\mathrm{MeV}/c$. The p_T resolution is $\sigma_{p_T}/p_T = (0.13\,(\mathrm{GeV})^{-1} \cdot p_T + 0.45)\%$. The ionisation energy loss (dE/dx) is measured by the two systems, with a resolution of approximately 14% and 7%, for the SVT and DCH, respectively. Additional particle identification information is provided by a Detector of Internally-Reflected Cherenkov light (DIRC), which, as described later, is employed in this analysis to provide a veto.

Hadronic events are selected by a filter which requires greater than two reconstructed tracks and a ratio of second to zeroth Fox-Wolfram moments [13] less than 0.98. The reconstructed momentum of the candidate tracks is corrected by $0.019(\,\mathrm{GeV}/c)^3/p^2$ to account for the underestimation of energy loss due to the pion mass assumption employed in the track fit. Candidates are retained only if they are within the full polar angle acceptance of the DCH ($-0.80 \le \cos\theta_{\mathrm{LAB}} \le 0.92$) and within $0.5 \le p_{\mathrm{LAB}} \le 1.5\,\mathrm{GeV}/c$, where the most probable dE/dx of d and $\overline{d}$ is well separated from that of other particle species. Here and throughout this Letter "LAB" denotes observables in the laboratory frame. To reject candidates with poorly-measured dE/dx, we require that the ionization along the track trajectory be sampled at least 24 times by the DCH. A relevant background contribution to the observed $\overline{d}$ signal comes from "secondary" d's produced in nuclear interactions with the detector material that travel inward toward the IP and are wrongly reconstructed as outward-travelling $\overline{d}$'s. To suppress this contribution we require that the transverse distance of closest approach (DOCA) of the reconstructed trajectory to the beamspot be less than 400 μm. The effect of underestimated energy loss on the measured DOCA of tracks is found to be well reproduced in the simulation, and we do not apply any correction to this quantity. Finally, d's and $\overline{d}$'s in the considered momentum range are below the threshold for radiating Cherenkov light in the DIRC quartz-glass bars, so we reject all the candidates with more than 10 associated Cherenkov photons for the the best-fit DIRC mass hypothesis, π, K, p, e or μ.

To measure the $\overline{d}$ yields, we apply a weight to each candidate to correct for detector and selection acceptance, and we then extract the yields from the $\overline{d}$ candidate energy loss distributions of the DCH and SVT using a weighted fit. Global trigger and event selection efficiencies are determined from simulated $e^+e^- \to Y \to 2(N\overline{N})X$ events, where X corresponds to zero or more additional final-state particles, and $Y = \Upsilon(2S)$, $\pi^+\pi^-\Upsilon(1S)$, or $q\overline{q}$ in which the nucleons are produced promptly in fragmentation. Those efficiencies are assumed to be the same for $\Upsilon(2S)$, $\Upsilon(3S)$, and $\Upsilon(4S)$, so only the first is explicitly calculated and used also for the other resonances. Corrections for the kinematic selections are computed as a function of p_{CM} using the fraction of $\overline{d}$, in bins of CM momentum, which would pass the selection in the LAB frame. This fraction depends on the angular distribution of $\overline{d}$'s in the CM frame with respect to the beam axis, which we determine from MC generator coalescence studies with coalescence momentum $p_0 = 160\,\mathrm{MeV}/c$ following a similar approach to [1]. Decays of $\Upsilon \to ggg$ produce d's and $\overline{d}$'s isotropically, while in $e^+e^- \to q\overline{q}$ there is a dependence on the CM polar angle.

The $\overline{d}$ reconstruction efficiency is determined in bins of p_{LAB} and $\cos\theta_{\mathrm{LAB}}$ from the "signal" MC samples. We compute an additional correction to this efficiency to account for the differing interactions of $\overline{d}$ and d in the material of the *BABAR* detector. Starting from the differing reconstruction probabilities of protons and antiprotons, as determined by GEANT4 simulation of $\Upsilon(nS)$ decays, we estimate the effect of material interaction on d and $\overline{d}$ by rescaling for the larger $\overline{d}$ absorption cross sections, determined in Ref. [14]. As a cross-check on the result, the values obtained at $\cos\theta_{\mathrm{LAB}} = 0$ are found to be consistent with a prediction obtained from $\overline{d}$ inelastic cross sections from Ref. [15] and the known distribution of material in the *BABAR* detector. The final weight applied to each track is the inverse of the product of the trigger and event selection efficiencies, the kinematic acceptance fraction, and the $\overline{d}$ reconstruction efficiency.

Yields are computed using a fit to the distribution of the normalized residual of ionization energy loss. Specific ionization measurements from the DCH and SVT, their uncertainties, and their expected values from the Bethe-Bloch formula are calibrated using high-statistics control samples of particles of other species. The independent dE/dx measurements, in arbitrary units, from the DCH and SVT are averaged according to their respective uncertainties, after rescaling the SVT measurement and its uncertainty such that the expected value matches that of the DCH. The normalized residual is computed as the difference between the averaged dE/dx measurement and the expected value, divided by the uncertainty of the former. Ideally, this residual (shown in Fig. 1 for $\Upsilon(2S)$

data) has a Gaussian distribution centered at zero for d's and $\overline{d}$'s, while the value for other species is far from zero (the value is positive or negative for particles with higher or lower mass, respectively).

The probability density function (p.d.f.) for d's and $\overline{d}$'s is estimated using signal MC events, while the distribution for all other particles is taken from the distribution for negatively-charged particles for the simulated generic decays of $\Upsilon(nS)$, which contain no true $\overline{d}$. The signal distribution is found to be well-modeled by a piecewise combination of a Gaussian function with an exponential tail toward lower values. After requiring that the piecewise function and its first derivative be continuuous, the addition of the tail adds only a single parameter as compared to a pure Gaussian. The residual distribution for other particles ("background") is more complicated, and extends into the signal region. This background distribution, obtained from simulated $\Upsilon(2S)$ events, is described well by the sum of a Gaussian function and an exponential function. Only the functional forms of the shapes used are extracted and validated using the MC samples, while almost all the p.d.f. parameters are estimated in the fit to the data. Very few candidates with large weights are removed since they could have an undue influence on the weighted fit [16]. An example of the fit to the residuals distribution for the $\overline{d}$ in the $\Upsilon(2S)$ data is shown in Fig. 1. For positively charged candidates we additionally

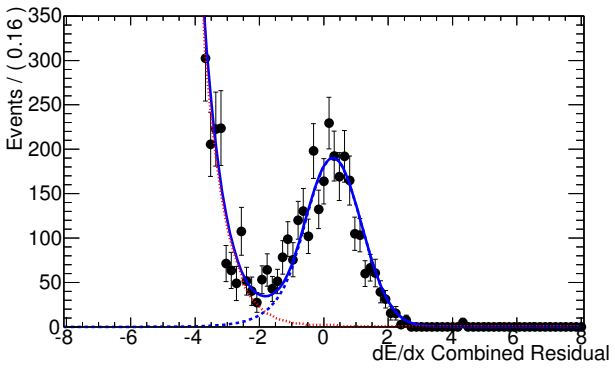

FIG. 1. Normalized residuals of the combined dE/dx for antideuteron candidates in the Onpeak $\Upsilon(2S)$ data sample, with fit p.d.f.'s superimposed. Entries have been weighted, as detailed in the text. The solid (blue) line is the total fit, the dashed (blue) line is the $\overline{d}$ signal peak, and the dotted (red) line is the background.

find a contribution from triton produced in material interactions. The tritons' distribution is similar to that of the d's and $\overline{d}$'s, so it is modeled using the same distribution with parameters allowed to float separately.

Candidates are divided into categories according to their charge, their CM momentum, and the type of dataset (Onpeak or Offpeak), and a weighted unbinned maximum likelihood fit is performed to all categories simultaneously. The d, $\overline{d}$, triton and background distribution functions are the same for all categories, but the yields are floated separately. We divide the CM momentum range [0.35,2.25] GeV/c into nine bins containing approximately equal numbers of candidates, with no bin narrower than 100 MeV/c. To improve the quality of the fit the width of the Gaussian function for the background is also allowed to float separately for different bins of CM momentum, to account for significant difference in the distribution for different energy ranges. To achieve a more stable fit, if the fit results for a split parameter (i.e., one allowed to take different values in different sub-samples) are statistically compatible between two or more sub-samples, the parameter is forced to have the same floating value among those sub-samples. We perform a simultaneous fit to Onpeak and Offpeak datasets for $\Upsilon(2S)$ and $\Upsilon(3S)$, obtaining the number of $\overline{d}$ in each CM momentum bin. Yield values and their uncertainties in each bin are reported in Ref. [17]. We determine the final number of $\overline{d}$ by subtracting the yields for $\overline{d}$ in the Offpeak dataset from the Onpeak, after rescaling for the luminosity and the lowest-order $1/s$ correction of the $e^+e^- \to q\overline{q}$ cross section.

The $\Upsilon(4S)$ decays almost exclusively to $B\overline{B}$ final states, and $\overline{d}$ production in B decays is kinematically disfavored, so the production from $\Upsilon(4S)$ decays is well below our sensitivity. Therefore, we proceed by combining the yields from Onpeak and Offpeak datasets to obtain the production rate for $e^+e^- \to q\overline{q}$. As a cross-check, when subtracting the rescaled yields in the Offpeak dataset from the yields in the Onpeak one, the number of $\overline{d}$'s are compatible with zero in all bins.

To extract the yields in $\Upsilon(1S)$ decay, we exploit candidates from $\Upsilon(2S) \to \Upsilon(1S)\pi^+\pi^-$ decays. We fit the Onpeak $\Upsilon(2S)$ dataset separately in two regions of recoiling invariant mass, $m_{\rm recoil} = \sqrt{(E_{\rm beam} - E_{\pi^+\pi^-})^2 - (\vec{p}_{\rm beam} - \vec{p}_{\pi^+\pi^-})^2}$: [9.453, 9.472] GeV/$c^2$ (signal) and [9.432, 9.452] GeV/c^2 plus [9.474, 9.488] GeV/c^2 (sidebands), and we subtract the yields in the sidebands, rescaled by their relative ranges, from those in the signal range. Due to lower statistics we use only five bins in CM momentum for this measurement.

Corrections due to the requirement on the number of DCH dE/dx samplings can be computed by comparing the distribution for this variable in data and signal simulation for d's in a narrow signal window that provides a clean and high-statistics control sample. We correct the fitted yields by -7% to account for this effect, which is not dependent on the CM momentum or polar angle.

To validate the fit procedure and check for possible biases in the $\overline{d}$ yields, we perform a series of fits to pseudo-datasets generated according to the fit p.d.f.'s and we assign a systematic uncertainty based on any bias found (i.e., the deviation from zero of the mean of the normalized residuals distribution). The uncertainty from our choice of the background model distribution function is

estimated by comparing to results obtained using a background model consisting of two Gaussian functions fixed to a common mean. Additional systematic uncertainties result from the weights used to correct for reconstruction efficiency in the detector and kinematic acceptance. We evaluate the effect of finite Monte Carlo statistics by allowing the weights to vary according to a Gaussian distribution centered at the nominal value with the width given by the uncertainties in the weights. We assign uncertainties in each bin from the distribution of fit results. The uncertainty in the correction for $\overline{d}$ material interaction is computed similarly, with the width of the Gaussian distribution set to the statistical uncertainty in the calculation plus the uncertainty assuming the correction distributed uniformly.

We estimate the contribution from secondary d's, described above, by fitting the DOCA distributions for data and simulated events in and outside the selected region. The simulation describes the data except for a slowly falling exponential component, which we ascribe to secondary d's. The fits indicate a small contribution to the selected events, which we take as a one-sided systematic uncertainty. We compare DOCA distributions of simulated antiprotons with a control sample of well-identified antiprotons and we assign a $+5.8\%$ one-sided uncertainty. The uncertainty in the event selection efficiency is estimated by comparing the nominal efficiency with the efficiency for events for which at least one of the generated prompt (anti)nucleons is a (anti)proton within the detector angular acceptance. Finally, uncertainties in the cross sections and number of $\Upsilon(nS)$ mesons are propagated along with the other systematics. The contributions to the systematic uncertainties are summed in quadrature separately for the positive and negative sides, and their values for each contribution and the totals are summarized in Table II. Systematic values in each bin are reported in Ref. [17].

The numbers of $\overline{d}$'s extracted from the fit are corrected for the differences between data and MC samples mentioned above, and then are converted into branching fractions for $\Upsilon(2S)$ and $\Upsilon(3S)$ using the total number of Υ decays. Using the total luminosity from Onpeak and Offpeak $\Upsilon(4S)$ datasets, we compute the cross section for $\overline{d}$ production from $e^+e^- \to q\overline{q}$ at a CM energy of $\approx 10.58\,\mathrm{GeV}$.

The number of $\Upsilon(1S)$ decays is computed as

$$N_{\Upsilon(1S)} = N^{\mathrm{fit}}_{\Upsilon(1S)} \times \frac{f_{\mathrm{sig}} - f_{\mathrm{sb}}}{\varepsilon_{\mathrm{filter}}}, \qquad (1)$$

where $N^{\mathrm{fit}}_{\Upsilon(1S)}$ is the number of $\Upsilon(2S) \to \pi\pi\Upsilon(1S)$ events reconstructed inclusively, obtained by a fit to the invariant mass recoiling against a reconstructed $\pi^+\pi^-$ system in $\Upsilon(2S)$ data. The quantities f_{sig} and f_{sb} are respectively the fraction of the fitted $\Upsilon(1S)$ recoil mass distribution in the signal and sideband regions used to subtract the contribution from background events, and $\varepsilon_{\mathrm{filter}}$ is the average efficiency of the trigger and the event filter to accept $\Upsilon(2S) \to \pi\pi\Upsilon(1S)$ decays obtained from the $\Upsilon(2S)$ MC sample. After applying these factors, we find $N_{\Upsilon(1S)} = (9.670 \pm 0.023) \times 10^6$. The final values for the differential branching fractions and $e^+e^- \to q\overline{q}$ cross section are shown in Fig. 2.

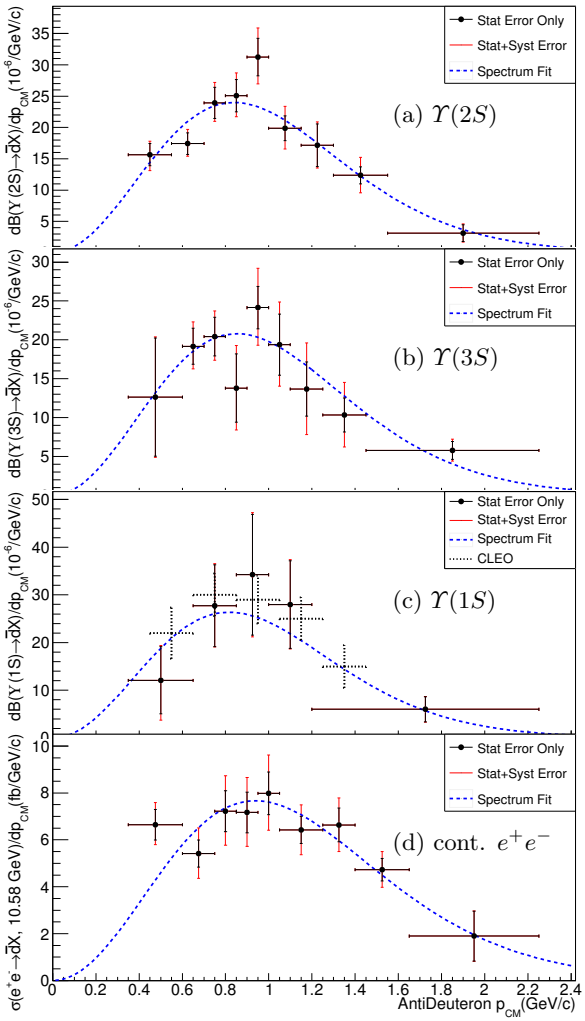

FIG. 2. Measured antideuteron differential spectra in (a) $\Upsilon(2S)$, (b) $\Upsilon(3S)$, (c) $\Upsilon(1S)$ decays, and (d) $e^+e^- \to q\overline{q}$ at a CM energy of $\approx 10.58\,\mathrm{GeV}$. The points with inner (black) error bars give the measurements and their associated statistical uncertainties, the outer (red) error bars give the quadratic sum of the statistical and systematic uncertainties, and the dashed (blue) curves show the fit to Eq. 2. Subfig. (c) also includes the CLEO results with dashed error bars for comparison.

The total rates, presented in Table III, are obtained from the measured differential spectra by fits to the "fireball" model distribution [18]

$$P(E) = \alpha v^2 e^{-\beta E}, \qquad (2)$$

where E is the $\overline{d}$ CM energy and α and β are free parameters determined by the fit. The fits are shown in

TABLE II. Contributions to the systematic uncertainties for the different measurements. Ranges are indicated where the contribution is different for each CM momentum bin.

Source	$\Upsilon(2S)$	$\Upsilon(3S)$	$\Upsilon(1S)$	Continuum
Fit Biases	0.5% — 2.0%	0.1% — 6.6%	0.1% — 2.0%	0.0% — 0.2%
Background Model	0.2% — 7.8%	3.1% — 12.0%	0.9% — 7.6%	0.0% — 8.9%
Reconstruction Efficiency	2.5% — 10.5%	5.2% — 17.0%	1.3% — 7.1%	3.0% — 7.3%
Kinematic Acceptance	0.5% — 10.3%	3.6% — 16.0%	0.6% — 2.9%	1.4% — 8.4%
Material Interaction	2.8% — 10.5%	4.3% — 17.0%	2.0% — 7.3%	2.9% — 7.4%
Fake antideuterons	$^{+0.0\%}_{-0.5\%}$ — $^{+0.0\%}_{-9.8\%}$	$^{+0.0\%}_{-1.1\%}$ — $^{+0.0\%}_{-3.0\%}$	$^{+0.0\%}_{-1.9\%}$ — $^{+0.0\%}_{-32.0\%}$	$^{+0.0\%}_{-0.6\%}$ — $^{+0.0\%}_{-5.4\%}$
DOCA Selection	$^{+5.8\%}_{-0.0\%}$	$^{+5.8\%}_{-0.0\%}$	$^{+5.8\%}_{-0.0\%}$	$^{+5.8\%}_{-0.0\%}$
Event Selection	2.3%	2.3%	1.1%	4.6%
Normalization	1.2%	1.2%	0.2%	0.6%

TABLE III. Total rates of antideuteron production. The first uncertainties listed are statistical, the second systematic. For comparison, we also list the ratio of our measurement of the inclusive antideuteron cross section to the cross section for hadronic production at a similar energy evaluated from [19].

Process	**Rate**
$\mathcal{B}(\Upsilon(3S) \to \bar{d}X)$	$(2.33 \pm 0.15^{+0.31}_{-0.28}) \times 10^{-5}$
$\mathcal{B}(\Upsilon(2S) \to \bar{d}X)$	$(2.64 \pm 0.11^{+0.26}_{-0.21}) \times 10^{-5}$
$\mathcal{B}(\Upsilon(1S) \to \bar{d}X)$	$(2.81 \pm 0.49^{+0.20}_{-0.24}) \times 10^{-5}$
$\sigma(e^+e^- \to \bar{d}X)$ $[\sqrt{s} \approx 10.58\,\mathrm{GeV}]$	$(9.63 \pm 0.41^{+1.17}_{-1.01})$ fb
$\dfrac{\sigma(e^+e^- \to \bar{d}X)}{\sigma(e^+e^- \to \mathrm{Hadrons})}$	$(3.01 \pm 0.13^{+0.37}_{-0.31}) \times 10^{-6}$

Fig. 2. The total rates quoted in Table III are the integral of these distributions from $0\,\mathrm{GeV}/c$ to $4\,\mathrm{GeV}/c$, and the associated uncertainties are those in the integral taking into account the full covariance of α and β. We find that values for the parameter β in Υ decays are mutually compatible within 1σ, and the average value is $\beta = (4.71 \pm 0.19)\,\mathrm{GeV}^{-1}$. Fitting to the $e^+e^- \to q\overline{q}$ spectrum yields a lower value of $(3.92 \pm 0.22)\,\mathrm{GeV}^{-1}$, corresponding to a somewhat harder spectrum. As an additional cross-check on the cross section for $e^+e^- \to q\overline{q}$ production, we fit separately the differential spectra from the $\Upsilon(4S)$ Offpeak dataset only, and obtain a cross section of $12.2 \pm 1.8\,\mathrm{fb}$, where the error is statistical only. Values for both this cross section and other parameters of the fit are in good agreement with the Onpeak plus Offpeak result.

In summary, we have performed measurements of inclusive $\overline{d}$ production in $\Upsilon(1,2,3S)$ decays and in $e^+e^- \to q\overline{q}$. These are the first measurements of $\overline{d}$ production in $e^+e^- \to q\overline{q}$ at a CM energy of $\approx 10.58\,\mathrm{GeV}$ and in $\Upsilon(3S)$ decay, and the most precise measurement in $\Upsilon(2S)$ decay. Our total and differential rates for inclusive $\bar{d}$ production in $\Upsilon(1S)$ and $\Upsilon(2S)$ decay are in good agreement with previous measurements [15], and with the expected spectral shapes from the coalescence model [20, 21]. We additionally note an order of magnitude suppression of $\overline{d}$ production in quark-dominated $e^+e^- \to q\overline{q}$ relative to the gluon-dominated Υ decays.

We are grateful for the excellent luminosity and machine conditions provided by our PEP-II colleagues, and for the substantial dedicated effort from the computing organizations that support *BABAR*. The collaborating institutions wish to thank SLAC for its support and kind hospitality. This work is supported by DOE and NSF (USA), NSERC (Canada), CEA and CNRS-IN2P3 (France), BMBF and DFG (Germany), INFN (Italy), FOM (The Netherlands), NFR (Norway), MES (Russia), MICIIN (Spain), STFC (United Kingdom). Individuals have received support from the Marie Curie EIF (European Union), the A. P. Sloan Foundation (USA) and the Binational Science Foundation (USA-Israel).

[a] Now at the University of Tabuk, Tabuk 71491, Saudi Arabia
[b] Also with Università di Perugia, Dipartimento di Fisica, Perugia, Italy
[c] Now at Laboratoire de Physique Nucléaire et de Hautes Energies, IN2P3/CNRS, Paris, France
[d] Now at the University of Huddersfield, Huddersfield HD1 3DH, UK
[e] Deceased
[f] Now at University of South Alabama, Mobile, Alabama 36688, USA
[g] Also with Università di Sassari, Sassari, Italy
[h] Also with INFN Sezione di Roma, Roma, Italy
[i] Now at Universidad Técnica Federico Santa Maria, Valparaiso, Chile 2390123

[1] Y. Cui, J. D. Mason, and L. Randall, JHEP **1011**, 017 (2010).
[2] L. A. Dal and M. Kachelriess, Phys. Rev. D **86**, 103536 (2012).
[3] A. Vittino, N. Fornengo, and L. Maccione, arXiv:1308.4848.
[4] H. Albrecht *et al.*, (ARGUS Collaboration), Phys. Lett.

B **236**, 102 (1990).
[5] D. M. Asner *et al.*, (CLEO Collaboration), Phys. Rev. D **75**, 012009 (2007).
[6] S. Schael *et al.*, (ALEPH Collaboration), Phys. Lett. B **639**, 192 (2006).
[7] J. Lees *et al.*, (*BABAR* Collaboration), Nucl. Instrum. Meth. A **726**, 203 (2013).
[8] T. Sjostrand, Comput. Phys. Commun. **82**, 74 (1994).
[9] D. Lange, Nucl. Instrum. Meth. A **462**, 152 (2001).
[10] S. Agostinelli *et al.*, (GEANT4 Collaboration), Nucl. Instrum. Meth. A **506**, 250 (2003).
[11] B. Aubert *et al.*, (*BABAR* Collaboration), Nucl. Instrum. Meth. A **479**, 1 (2002).
[12] B. Aubert *et al.*, (*BABAR* Collaboration), Nucl. Instrum. Meth. A **729**, 615 (2013).
[13] G. C. Fox and S. Wolfram, Phys. Rev. Lett. **41**, 1581 (1978).
[14] S. Denisov *et al.*, Nucl. Phys. B **31**, 253 (1971).
[15] J. Beringer *et al.*, (Particle Data Group), Phys. Rev. D **86**, 010001 (2012).
[16] F. James, *Statistical Methods in Experimental Physics*, 2nd ed. (World Scientific, 2006).
[17] See Supplemental Material at [URL will be inserted by publisher] for additional data.
[18] R. Hagedorn, Nucl. Phys. B **24**, 93 (1970).
[19] R. Giles *et al.*, Phys. Rev. D **29**, 1285 (1984).
[20] H. H. Gutbrod *et al.*, Phys. Rev. Lett. **37**, 667 (1976).
[21] H. Sato and K. Yazaki, Phys. Lett. B **98**, 153 (1981).